

Topology of Two-Dimensional Turbulence

W. Brent Daniel^{1,2,*} and Maarten A. Rutgers¹

¹*Department of Physics, The Ohio State University, Columbus, Ohio 43210*

²*Condensed Matter and Thermal Physics Group and the Center for Nonlinear Studies, Los Alamos National Laboratory, Los Alamos, New Mexico 87545*

(Received 17 April 2002; published 10 September 2002)

Velocity differences in the direct enstrophy cascade of two-dimensional turbulence are correlated with the underlying flow topology. The statistics of the transverse and longitudinal velocity differences are found to be governed by different structures. The wings of the transverse distribution are dominated by strong vortex centers, whereas the tails of the longitudinal differences are dominated by saddles. Viewed in the framework of earlier theoretical work, this result suggests that the transfer of enstrophy to smaller scales is accomplished in regions of the flow dominated by saddles.

DOI: 10.1103/PhysRevLett.89.134502

PACS numbers: 47.27.Gs

Two-dimensional (2D) turbulence is a fascinating problem with relevance in areas as wide ranging as the dynamics of energy transfer in atmospheric and geophysical flows [1] to the basic statistical mechanics of interacting vortices [2–4]. Three decades of theoretical and numerical work starting from the seminal ideas of Kraichnan [5] and Batchelor [6] have provided a picture of 2D turbulence based upon the scaling laws of abstract statistical quantities. This description remains strikingly incomplete. For example, there is still no clear physical understanding of the mechanisms by which energy and enstrophy are transferred between different length scales in a turbulent flow; nor is there a conclusive picture of how the intense coherent structures that dominate the statistics are formed and evolve.

The challenge is to establish a connection between the statistical measures of turbulence and the physical dynamics of the turbulent flow field. In the current work, we demonstrate that, by considering correlations between local flow topology [7,8] and velocity difference probability distributions (PDFs) [9–13], we can make this important connection. The wings of the distributions of the transverse and longitudinal velocity differences are found to be associated with very different structures: vortex centers and saddles, respectively. As a consequence, it will turn out that the transfer of enstrophy must be accomplished near saddle points. This transfer is the result of a topological asymmetry in the turbulent flow manifest in the longitudinal velocity difference PDFs. Furthermore, since the wings of the longitudinal velocity differences are dominated by strong saddles, a complete understanding of intermittency in 2D must include a motivation for the formation of these structures. This powerful technique can be extended to other statistical quantities to infer correlations between flow topology and turbulent dynamics.

Local flow topology is characterized by the four first-order derivatives in the expansion of the vector velocity,

$$\hat{m} = \begin{pmatrix} \partial_x v_x & \partial_y v_x \\ \partial_x v_y & \partial_y v_y \end{pmatrix}. \quad (1)$$

The determinant of this Jacobian matrix,

$$\Lambda = \det(\hat{m}) = \frac{1}{4}(\omega^2 - \sigma^2), \quad (2)$$

represents a local balance between the vorticity and strain rate. Using this measure, the flow field can be partitioned into strain-dominated regions (saddles) and vorticity-dominated regions (centers). This partitioning is commonly called the Okubo-Weiss criteria. Rivera, Wu, and Yeung [14] showed that the probability distribution of the Jacobian determinant is nonanalytic at $\Lambda = 0$, since centers and saddles are topologically distinct, and asymmetric, with vortex centers being significantly more likely than saddles of comparable strength; see Fig. 1(a).

A statistical correlation between the local flow topology characterized by Λ and the velocity differences is constructed from data obtained from a 2D flowing soap film experiment, the configuration of which is described in Ref. [15] with an effective injection scale of 2 cm. The Jacobian determinant at each location is calculated from the matrix, \hat{m} , averaged over a disk, Ω , with a center halfway between the two velocity measurements and radius, r_Ω , equal to $r/2$. That is, $\hat{\Lambda} = \det(\hat{M})$, where

$$M^{\alpha\beta} = \frac{\int_\Omega m^{\alpha\beta} dA}{\int_\Omega dA}. \quad (3)$$

By performing the average in this manner, a scale dependence of the quantity is maintained, allowing the method to probe different regions of the enstrophy cascade. Here, however, we will be reporting results for only one separation, $r = 0.4$ cm. This average over the smaller scales in the flow is permissible in the enstrophy cascade since enstrophy transfer through a given scale depends only on larger scales and not on these smaller structures [16].

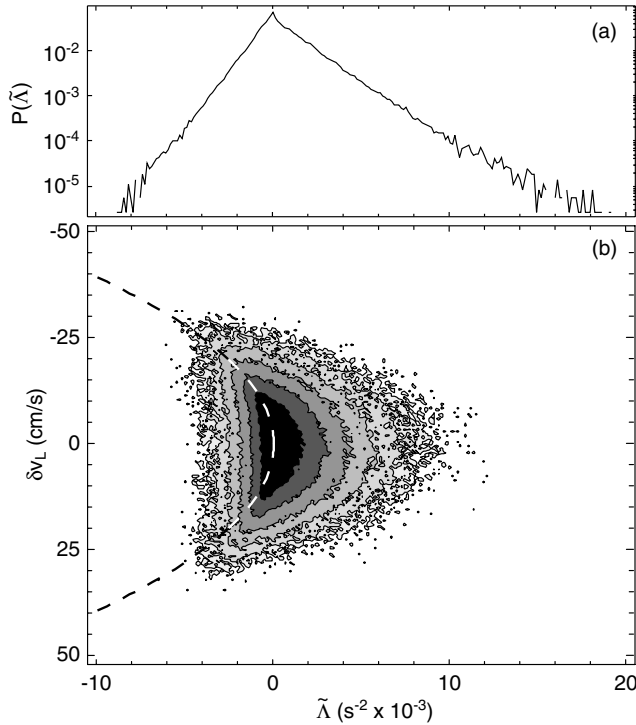


FIG. 1. (a) The asymmetric distribution of the Jacobian determinant, $P(\tilde{\Lambda})$. (b) Multivariate probability distribution, $P(\tilde{\Lambda}, \delta v_L(r = 0.4 \text{ cm}))$, indicating the likelihood that a given longitudinal velocity difference will be found in a region of the flow with topology described by $\tilde{\Lambda}$. The dashed line indicates the velocity difference of maximum likelihood. Note that the direction of increasing velocity difference along the vertical axis is nonstandard. Shading and contours represent the log of the probability.

There is some sensitivity to flow inhomogeneities in this measurement since we are averaging over a macroscopic region of the flow. The inhomogeneity is characterized by a 25% variation in the turbulence intensity across the 2.0 cm wide measurement area. This variation is due to the particular turbulent forcing mechanism used (a pair of combs arranged in an inverted wedge [17]). Nevertheless, over a 0.28 cm wide stripe down the central region of the channel where we gather statistics, the turbulence intensity varies by less than 1%. Further, a simple line average between the two points at which the velocity is measured—less affected by cross-stream inhomogeneity—produced the same results.

A rigorous connection between the abstract velocity difference statistics and the concrete flow topology is established through multivariate probability distributions of the form $P(\tilde{\Lambda}, \delta v_i(r))$, where i represents either the transverse, T , or longitudinal component, L , of the velocity difference. The form of these distributions differs significantly between the longitudinal and transverse velocity increments as a result of the different symmetries of the saddle and center; see Figs. 1 and 2. The wings of the longitudinal velocity difference PDF are dominated

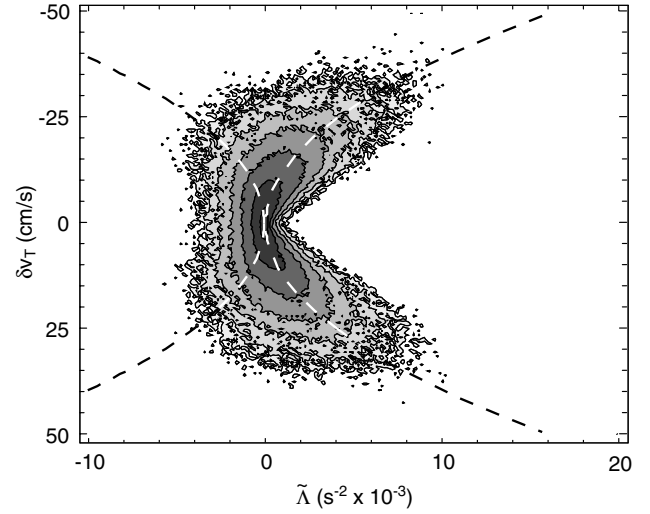


FIG. 2. Multivariate distribution, $P(\tilde{\Lambda}, \delta v_T(r = 0.4 \text{ cm}))$, indicating the likelihood of finding a given transverse velocity difference in a region of the flow with topology described by $\tilde{\Lambda}$. The dashed lines indicate the velocity difference of maximum likelihood.

by strong saddles, whereas the wings of the transverse velocity difference are dominated by strong centers. To understand the reason for this distinction, we examine the distribution of the velocity differences about these two first-order structures in some detail.

We begin with an examination of a saddle point. The symmetry of a saddle is such that the distribution of the longitudinal and transverse velocity differences about it is the same. If the matrix, \hat{m} , is parametrized as

$$\hat{m} = \frac{1}{\sqrt{2}} \begin{pmatrix} \lambda & \Delta + \omega \\ \Delta - \omega & -\lambda \end{pmatrix}, \quad (4)$$

the radial and angular components of the velocity about a saddle (described by the symmetric part of \hat{m}) are given by $v_r = [\lambda \cos(2\theta) + \Delta \sin(2\theta)]r$ and $v_\theta = [\lambda \sin(2\theta) - \Delta \cos(2\theta)]r$, respectively. As long as $\sigma^2 = \lambda^2 + \Delta^2$ is held constant, the relative magnitudes of λ and Δ serve only to vary the spatial orientation of the saddle. We can, therefore, make the simplifying assumption that the saddle is described by $\sigma^2 = \lambda^2$. Using $P(v_r(\theta)) \propto [\partial_\theta v_r(\theta)]^{-1}|_{\theta(v_r)}$ and $P(v_\theta(\theta)) \propto [\partial_\theta v_\theta(\theta)]^{-1}|_{\theta(v_\theta)}$ in the longitudinal and transverse cases, respectively, we obtain probability distributions of the form

$$P(\delta v_i(r) | \tilde{\Lambda}) = \frac{2}{\pi \sqrt{r^2 \tilde{\Lambda}^2 - \delta v_i^2}}, \quad (5)$$

regardless of which velocity increment is examined. Here we have let, for example, $\delta v_L = 2v_r$ and replaced the independent variables λ and Δ by an equivalent pair expressing the saddle strength, σ^2 , and orientation. Because of this similarity, it is not surprising that the appearance of the multivariate distributions, $P(\tilde{\Lambda}, \delta v_T(r))$ and

$P(\tilde{\Lambda}, \delta v_L(r))$, are, at first order, identical for $\tilde{\Lambda} \ll 0$ [where $\tilde{\Lambda} \approx -(1/4)\sigma^2$]. The velocity differences of maximum likelihood for a given saddle strength follow the curve $\delta v_i = \pm r\sqrt{-\tilde{\Lambda}}$ for $\tilde{\Lambda} < 0$, independent of which velocity difference is being considered [the dashed lines for $\tilde{\Lambda} < 0$ in Figs. 1(b) and 2]. Note that the assumption that the dominant topology takes the form of a saddle is not valid as $\tilde{\Lambda}$ nears zero. In this regime, Fig. 3 shows that the expected values of the squared strain rate and squared vorticity become of comparable magnitude. The form of the $P(\delta v_i(r) | \tilde{\Lambda})$ is, therefore, distorted as the topological features themselves are stretched.

Although the distributions of the longitudinal and transverse velocity differences are identical across a saddle, the distribution of these two quantities about a vortex center differs dramatically. Across an axisymmetric vortex center, the longitudinal velocity difference is precisely zero (since the radial component of the velocity itself is zero). For positive values of the Jacobian determinant, points in the distribution $P(\tilde{\Lambda}, \delta v_L(r))$ which lie away from $\delta v_L = 0$ do so either as the result of first-order contributions from the strain rate or through higher order corrections to the flow field. Since the magnitude of the longitudinal velocity difference across a vortex center is, thus, constrained to be small, it is saddlelike regions of the flow which play the dominant role in the wings of the longitudinal velocity difference PDFs and, correspondingly, in the higher order longitudinal structure functions.

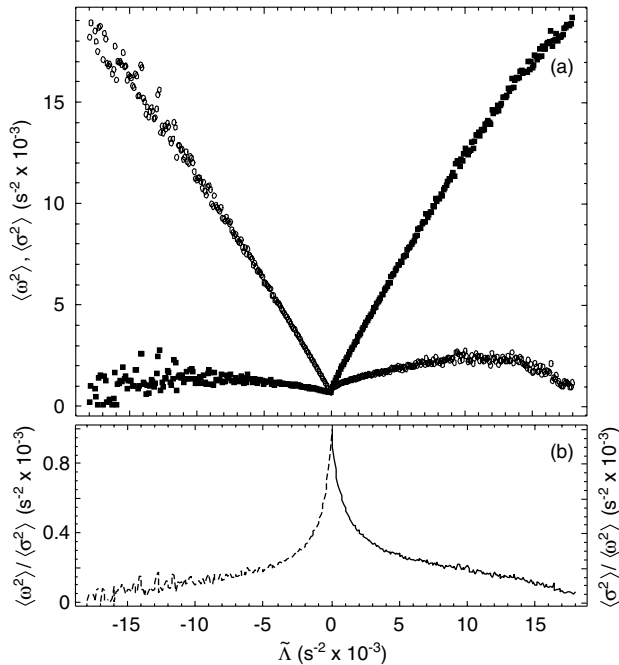


FIG. 3. (a) The expected values of $\langle \omega^2 \rangle$, filled squares, and $\langle \sigma^2 \rangle$, open circles. For positive and negative $\tilde{\Lambda}$, different topologies tend to be significantly dominant, as indicated by (b) the ratios $\langle \omega^2 \rangle / \langle \sigma^2 \rangle$ (dashed line) and $\langle \sigma^2 \rangle / \langle \omega^2 \rangle$ (solid line) for negative and positive $\tilde{\Lambda}$, respectively.

A clear picture of intermittency in 2D must, therefore, include an understanding of the formation of unusually strong saddle points in addition to coherent vortex centers.

On the other hand, vortex centers do support significant *transverse* velocity differences. In fact, vortex centers with $\delta v_T = 0$ cannot exist as a consequence of Stokes' law: $\oint_C v_\theta r_\Omega d\theta = \int_\Omega \omega_z d\Omega$, where C traces the perimeter of the disk, Ω , and for $\tilde{\Lambda} > 0$, the sign of v_θ is the same about the entire perimeter. As the magnitude of the transverse velocity goes to zero, so must the magnitude of the vorticity. The shape of the distribution is obtained under the assumption that for locations in the flow with $\tilde{\Lambda} \gg 0$ the topology is dominated by the vorticity. Setting $\tilde{\Lambda} = (1/4)\omega^2$, $v_\theta = \omega r_\Omega$, $\delta v_T = 2v_\theta$, and letting $r_\Omega = r/2$, we find that the transverse velocity difference varies as a function of the local Jacobian determinant according to $\delta v_T = \pm r\sqrt{\tilde{\Lambda}}$ for $\tilde{\Lambda} > 0$ (the dashed line in Fig. 2). The finite spread in the distribution results both from higher order corrections to the shape of the vortex centers as well as from the fact that, in actuality, there are finite contributions from first-order saddles; that is, $\langle \sigma^2 \rangle / \langle e_s \rangle$ is of order 0.2 for $\tilde{\Lambda} > 0$.

Because of the larger propensity for strong vortex centers to form relative to saddle points of comparable magnitude [recall Fig. 1(a)], the maximum transverse velocity difference found about centers in the flow is significantly greater than that found about saddles (compare Fig. 2 for $\tilde{\Lambda} < 0$ and $\tilde{\Lambda} > 0$). The wings of the transverse velocity difference PDF in the enstrophy cascade are, therefore, dominated by contributions from vortex centers. Because of this clear segregation between the structures which play the dominant role in the transverse and longitudinal velocity differences, it would not be surprising if the higher order moments of these two quantities differed.

The characterization of the flow topology, $\tilde{\Lambda}$, can accurately reflect the Lagrangian evolution of the flow field, so long as the velocity gradients vary sufficiently slow [7,8]. A criterion proposed in Refs. [18,19] gives a quantitative measure of the validity of this assumption by taking into account the Lagrangian time derivative of the strain rates and vorticity. The bases of this criterion are the eigenvalues of the pressure Hessian given by $\lambda^{(\pm)} = \lambda_0 \pm \lambda_1$, where p is the pressure field, $\lambda_0 = -\tilde{\Lambda}$, and $\lambda_1 = (1/2)\sqrt{\tilde{\sigma}_n^2 + \tilde{\sigma}_s^2 - \tilde{\omega}^2}$ (n and s denote the normal and shear components, respectively). When the signs of both $\lambda^{(\pm)}$ are the same, $|\lambda_1|$ is smaller than $|\lambda_0|$ and the more straightforward characterization based on $\tilde{\Lambda}$ is valid. Figure 4 displays the multivariate distribution of $P(\lambda_0, \lambda_1)$. The strongest centers preferentially lie in the region of the distribution corresponding to both $\lambda^{(\pm)}$ negative. These are topological features about which the pressure field is relatively isotropic and, hence, features which are not rapidly deformed. Correspondingly, the assumption made by Okubo and Weiss is valid for these structures so that $\tilde{\Lambda}$ adequately characterizes the

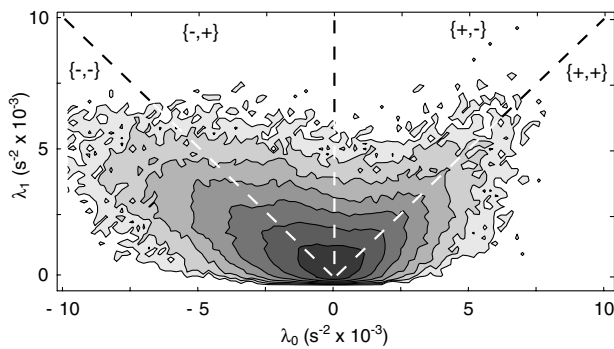


FIG. 4. Correlation between first and second terms of pressure Hessian eigenvalues, $\lambda^{(\pm)} = \lambda_0 \pm \lambda_1$; see Refs. [18,19] for details. The first term, $\lambda_0 = -\tilde{\Lambda}$, is trivially related to the Okubo-Weiss criterion. The second, λ_1 , quantifies the relative variation in the local strain rate and vorticity. Where the sign of both $\{\lambda^{(+)}, \lambda^{(-)}\}$ is the same the assumption made by Okubo and Weiss is valid.

underlying turbulent dynamics for $\tilde{\Lambda}$ large. In fact, the assumption is valid in 60% of all centerlike regions. On the other hand, there is a smaller fraction of saddles for which this is true, only 47%. However, $\tilde{\Lambda}$ is still an adequate characterization of the dynamics for $|\tilde{\Lambda}|$ sufficiently large. For example, 83% of saddles in which $|\tilde{\Lambda}| > 5000 \text{ s}^{-2}$ have $\lambda^{(\pm)}$ both positive. The tails of the distributions in Figs. 1 and 2 are, thus, accurate representations of the underlying dynamics.

The rudimentary observations presented so far have certainly not expended the usefulness of velocity and pressure topology as an analytical tool. It is, first of all, interesting that the ratio $\langle \sigma^2 \rangle / \langle \omega^2 \rangle$ tends toward zero for $\tilde{\Lambda} \gg 1$. This implies that the strongest vortex centers are nearly axisymmetric. This was not seen in the earlier continuously forced experiment of Rivera *et al.* [14]. These axisymmetric centers are the likely predecessors of the coherent structures found in the latter stages of 2D turbulent decay [3,4,12,20,21]. They are stable [20,22,23], steady-state solutions of the Euler equation in which there is no nonlinear transfer of enstrophy and, hence, no enstrophy cascade [24].

Furthermore, a key feature is still missing from the first-order distribution, $P(\delta v_L(r) | \tilde{\Lambda})$. It is a well known result in turbulence theory that the rate of enstrophy transfer, η , depends on an odd moment of the longitudinal velocity difference [25], $S_3^{(L)}(r) = (1/8)\eta r^3$, and, hence, on an asymmetry in the distribution of these velocity differences. This asymmetry is missing in Eq. (5), where $P(\delta v_L | \tilde{\Lambda}) = P(-\delta v_L | \tilde{\Lambda})$. It is, in fact, necessary to go to at least third order to explain the asymmetry in $P(\delta v_L)$, where it is possible to construct an asymmetric saddle, that is, one in which the magnitude of the velocity in the incoming and outgoing jets differs.

The longitudinal velocity difference about such a structure is asymmetric, whereas positive and negative transverse velocity increments persist with equal likelihood. A systematic correlation between these higher order topological structures and the velocity differences is beyond the limits of the current data set, but future work will explore these connections.

We thank Michael Rivera, Robert Ecke, and Michael Chertkov for many insightful conversations. The present work was supported by the Petroleum Research Foundation, The Ohio State University, and the U.S. Department of Energy (W-7405-ENG-36).

*Electronic address: wdaniel@lanl.gov

- [1] J. C. McWilliams, J. B. Weiss, and I. Yavneh, *Science* **264**, 410 (1994).
- [2] Y. Couder and C. Basdevant, *J. Fluid Mech.* **173**, 225 (1986).
- [3] R. Robert and J. Sommeria, *J. Fluid Mech.* **229**, 291 (1991).
- [4] J. Miller, *Phys. Rev. Lett.* **65**, 2137 (1990).
- [5] R. Kraichnan, *Phys. Fluids* **10**, 1417 (1967).
- [6] G. Batchelor, *Phys. Fluids B* **12**, 233 (1969).
- [7] A. Okubo, *Deep-Sea Res.* **17**, 445 (1970).
- [8] J. Weiss, *Physica (Amsterdam)* **48D**, 273 (1991).
- [9] U. Frisch, *Turbulence: The Legacy of A. N. Kolmogorov* (Cambridge University, Cambridge, 1995).
- [10] K. Sreenivasan, S. Vainshtein, R. Bhiladvala, I. San Gil, S. Chen, and N. Cao, *Phys. Rev. Lett.* **77**, 1488 (1996).
- [11] G. Eyink, *Physica (Amsterdam)* **91D**, 97 (1996).
- [12] L. Smith and V. Yakhot, *Phys. Rev. E* **55**, 5458 (1997).
- [13] P. Vorobieff, M. Rivera, and R. E. Ecke, *Phys. Fluids* **11**, 2167 (1999).
- [14] M. Rivera, X. L. Wu, and C. Yeung, *Phys. Rev. Lett.* **87**, 044501 (2001).
- [15] M. Rutgers, X. L. Wu, and W. B. Daniel, *Rev. Sci. Instrum.* **72**, 3025 (2001).
- [16] G. Falkovich and V. Lebedev, *Phys. Rev. E* **50**, 3883 (1994).
- [17] M. Rutgers, *Phys. Rev. Lett.* **81**, 2244 (1998).
- [18] B. L. Hua and P. Klein, *Physica (Amsterdam)* **113D**, 98 (1998).
- [19] C. Basdevant and T. Philipovitch, *Physica (Amsterdam)* **73D**, 17 (1994).
- [20] J. McWilliams, *J. Fluid Mech.* **146**, 21 (1984).
- [21] A. Bracco, J. C. McWilliams, G. Murante, A. Provenzale, and J. B. Weiss, *Phys. Fluids* **12**, 2931 (2000).
- [22] N. Whitaker and B. Turkington, *Phys. Fluids* **6**, 3963 (1994).
- [23] Y. Kimura and J. R. Herring, *J. Fluid Mech.* **439**, 43 (2001).
- [24] A. Babiano, C. Basdevant, B. Legras, and R. Sadourny, *J. Fluid Mech.* **183**, 379 (1987).
- [25] D. Bernard, *Phys. Rev. E* **60**, 6184 (1999).